

ORIGINAL ARTICLE

The Microstructure and Surface Roughness of Al–Si Alloys as–cast at Different Cooling Rates with Tin Addition

Hesham Elzanaty

Basic Engineering Sciences Department, Faculty of Engineering, Delta University for Science and Technology, Gamasa, Mansoura, Egypt

Corresponding Author Email: dr.hesham_aly@yahoo.com

Abstract: This paper attempts to investigate the effect of low melting point additives (tin) on the microstructure and surface roughness of Al–Si alloys and the role of cooling rates (9.6°C/s and 26.2°C/s) on the microstructure and surface roughness of Al–Si alloys. Tin has no effect on the Si morphology because Sn wets the Al grain boundaries. It can be discerned that a high cooling rate resulted in the refinement of both primary and eutectic Si particles. Surface roughness measurements and optically observed features on the finished surface give important information about the quality of the surface produced. According to that, Al–Si alloys with 1.0% Sn cast at a cooling rate 26.2°C/s at a speed, 0.92 m/s has smoothest surface and is good for bearing applications.

Keywords: Aluminium, Silicon, Al–Si alloys, Bismuth, Tin, Microstructure and surface roughness.

Introduction

In recent times non–ferrous metals and alloys have become so important that technological development without them is unconceivable. Among the most important non–ferrous metals is aluminium with its alloys. Aluminium excels among other non–ferrous metals because of its high specific weight, resistance to corrosion etc (Miller et al., 2000; Totten & Mackenzie, 2003). Aluminium and its alloys have been identified as an important and useful engineering material. It is attracted by its various unique properties; such as appearance, strength–to–weight ratio, excellent thermal properties, workability properties and good mechanical behaviour. Cast aluminium alloys are mostly grain refined by adding mixtures of some essential elements to enhance and impact some important characteristics (Samuel & Samuel, 1995; Jorstad, 2006; Tash et al., 2007). Aluminium is non–combustible, non–toxic and non–absorbent. At present the output of Aluminium by volume is greater than that of other non–ferrous metals. The ductility of aluminium in hot state enables almost any cross–sectional shape to be extruded easily. Addition of some elements to aluminium improves its properties, for example aluminium is most commonly extruded in the

alloyed form. The resistance of aluminium to corrosion is influenced by some elements and their percentages by weight alloyed to aluminium. Silicon is added to improve liquid fluidity in aluminium while copper improves its mechanical properties (Wang and C. H. Caceres, 1998; Gruzleski and B. M. Closset, 1990; Machovec et al., 2000; Rincón et al., 2007; Ammar et al., 2008; Yamagata et al., 2008; Chen et al., 2009).

Aluminium–Silicon alloys are the most commonly used alloys in the automotive, defense and aerospace industries mainly because of their high strength to weight ratios, better castability and good surface finish (Patel & Prajapati, 2012; Prashanth et al., 2013; Vandana et al. 2014; Elzanaty et al., 2015). Al–Si are the most widely used aluminium casting alloys on account of their superior castability properties, e.g. high fluidity, low shrinkage and low thermal expansion coefficient. Al–Si alloys are classified into three categories based on their silicon percentage: i) eutectic, ii) hypoeutectic, and iii) hypereutectic. Si particles appear as platelets or needle–like particles in hypoeutectic Al–Si alloys, while hypereutectic contains both the block–like primary Si phase particles and platelet or needle–like eutectic Si

particles. The very low solubility of silicon in aluminum means that Al–Si alloys contain virtually pure α -aluminum with silicon as either a primary (in hypereutectic alloy) or eutectic (in hypoeutectic or eutectic alloys) phase, depending on whether the silicon percentage is greater or less than the eutectic point (12.6 % Si), on the cooling rate, and on the concentration of modifiers added (Wang and C. H. Caceres, 1998; Yamagata et al., 2008). Minor additions of Sn, up to 0.1 % wt., increase the peak hardness of the alloys due to the enhanced formation of interdendritic structures. The presence of bismuth within the alloy enhances the lubricity of the alloy by essentially remaining as elemental bismuth within the alloy (Machovec et al., 2000; Cho & Loper, 2000; Koike et al., 2000; Chen et al., 2009). Structural modification can be achieved using various additives to modify the structure of Al–Si alloys. The size and shape of eutectic Si in hypoeutectic Al–Si alloys and of primary Si in hypereutectic Al–Si alloys have a great effect on the final mechanical properties of the manufactured parts. The modification of the Si morphology from flake-like to fibrous form was believed to greatly improve the mechanical properties. Al–Si alloys with high cooling rates have refined microstructures (Yamagata et al., 2008). The microstructures of Al–Si alloys can also be refined through melt treatment (Samuel and F. H. Samuel, 1995; Prashanth et al., 2013), Low-melting-point elements, such as Bi, Sn, Pb, and Cd all have an influence on the microstructure and properties of Al–Si alloys. Bismuth and tin are preferred additives for improving the dry machining performance of Al–Si alloys (Machovec et al., 2000; Cho & Loper, 2000; Koike et al., 2000; Emadi et al., 2006; Chen et al., 2009).

Surface quality of the machined surface is one of the most important concerns in a machining operation. Surface roughness measurements and optically observed features on the finished surface give important information about the quality of the surface produced and hence about the machinability of the given alloy under the conditions used for the process (Balaji & Jawahir, 2001; Nouari et al., 2003; Chen et al., 2009; Dasch et al., 2009). The surface roughness produced in turning depends on the feed rate, tool geometry, tool wear, and the material characteristics of the workpiece and the tool; it can be reduced by decreasing the feed rate and the depth of cut, increasing the cutting speed and the rake angle, and improving the workpiece material by adding free-machining additives or increasing the hardness (Patel & Prajapati, 2012; Prashanth et al., 2013; Vandana et al. 2014; Emadi et al., 2006).

Materials and Methods

Materials used for this research are: high purity aluminium, silicon, bismuth, tin, beakers, and electronic weighting balance. Cast Al–Si alloys (hypoeutectic and hypereutectic), which have extended applications in automotive components, were cast and cooled under different cooling rates (9.6°C/s and 26.2°C/s). The melt processes showed differences for the hypereutectic and hypoeutectic Al–Si alloys. For the hypoeutectic Al–Si alloys, the base hypoeutectic alloy had a composition of Al–6% Si. For the hypereutectic Al–Si alloys, the base hypereutectic alloy had a composition of Al–16% Si. Melts were prepared using high purity aluminium and silicon. Two different Bi concentrations of 0.5, and 1.0 wt.% and three different Sn concentrations of 0.25, 0.5, and 1.0 wt.% were used. The molten was poured to the steel casting mould and the copper mould, after being mixed in the bath manually, and holding for 15 minutes. This holding duration was necessary to allow the inclusions to drop to the bottom of melt, and make the final samples free of these inclusions, which are often ceramic particles. These inclusions may adversely affect the machinability. The molten alloy was then poured into the steel and copper moulds at 750°C. To obtain two different cooling rates, the permanent steel mould was preheated to 400°C to obtain a cooling rate of 9.6°C/s and the copper mould was maintained at room temperature to obtain a cooling rate of 26.2°C/s. The copper mould had a smaller cavity for the molten aluminum, and a thicker wall section. The microstructure of experimental casts was studied using an optical microscope and scanning electron microscope (SEM). Roughness measurements have been done using Surface roughness tester, Surftest SJ201P. The surface roughness value that was measured is expressed in terms of the Centre Line Average or the R_a value.

Results and Discussion

Microstructure

The goal of microstructural analysis is to develop a quantitative description of microstructure that can be used to establish its relationship to properties. The Al–Si casting alloys contain two principal phases: aluminum based α -Al as the phase with the largest volume fraction, acts as the matrix for the alloy, and the silicon phase, which is found largely in two forms: primary ‘blocky’ silicon and ‘plate like’ eutectic silicon (Elzanaty et al., 2015). The microstructure of the alloys depends on the composition of the two primary elements, aluminum and silicon. Figure 1 to figure 6 describes the microstructures of Al–Si alloys with different concentrations of tin produced at different

cooling rates. Hypoeutectic and hypereutectic alloys were made in order to understand the following points:

1. The effect of tin on the microstructure of Al–Si alloys.
2. The role of cooling rates on the microstructure of Al–Si alloys.

The micrograph of the Al–Si alloys with 0.5 % and 1.0 % Sn solidified under cooling rates 9.6 °C/s and 26.2 °C/s is shown in figure 1 to figure 6. Primary aluminum dendrites and eutectic silicon particles were present in the microstructure of the base alloys. The particles of pure Sn were not present in the form of spherical particles, because

it tended to form a film on the boundaries of the Al grains or at the interface of Al and Si. The grey phase seen in the microscopy images is the eutectic Si particles in fine spherical morphology, and Sn has no strong effect on the silicon morphology at different cooling rates. The amount of Sn at the interface of Al–Si was slightly higher in the alloys with 1.0 % modification than that in alloys with 0.5 % modification. The quantitative results indicate that the cooling rate plays a significant role in the refinement of the microstructure. It can be discerned that, at high cooling rate resulted in the refinement of both primary and eutectic Si particles. The sizes of the Si particles of the alloys cast with a cooling rate of 26.2 °C/s are smaller than those of the alloys cast with a cooling rate of 9.6 °C/s.

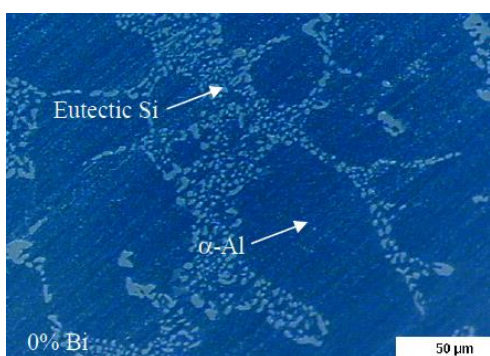


Figure 1. Microstructure of Al–Si Alloy with 0.0% Sn as cast at cooling rate of 9.6°C/s.

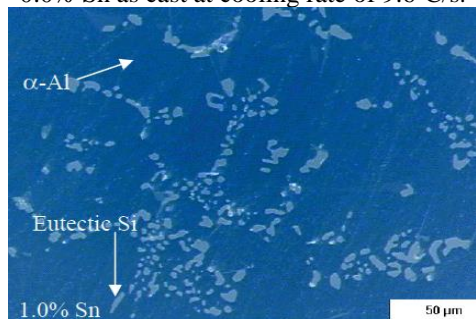


Figure 3. Microstructure of Al–Si Alloy with 1.0% Sn as cast at cooling rate of 9.6°C/s.

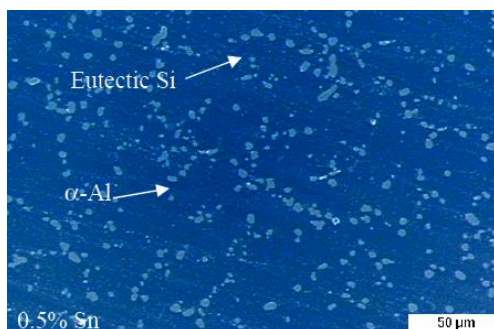


Figure 5. Microstructure of Al–Si Alloy with 0.5% Sn as cast at cooling rate of 26.2°C/s.

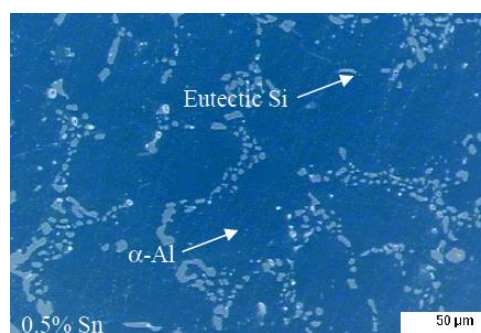


Figure 2. Microstructure of Al–Si Alloy with 0.5% Sn as cast at cooling rate of 9.6°C/s.

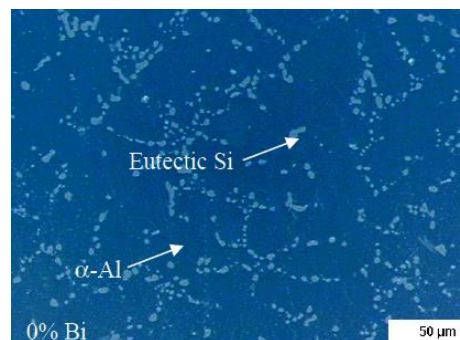


Figure 4. Microstructure of Al–Si Alloy with 0.0% Sn as cast at cooling rate of 26.2°C/s.

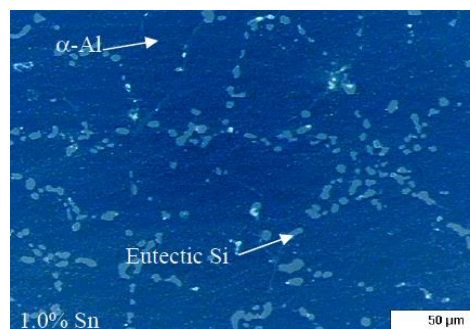


Figure 6. Microstructure of Al–Si Alloy with 1.0% Sn as cast at cooling rate of 26.2°C/s.

Surface Roughness

The roughness is an important parameter for bearing materials. The roughened crankshaft may in turn cause wear of the bearings. Not only roughness of the surface but also dirt entering the bearing clearance with the oil flow is a source of

bearing damage. The surface roughness parameter (average roughness height, R_a) of Al-Si cast alloys at different cooling rates is shown in figure 7 to figure 10. According to that, Al-Si alloys with 1.0% Sn cast at a cooling rate 26.2°C/s at a speed, 0.92 m/s has smoothest surface and is good for bearing applications.

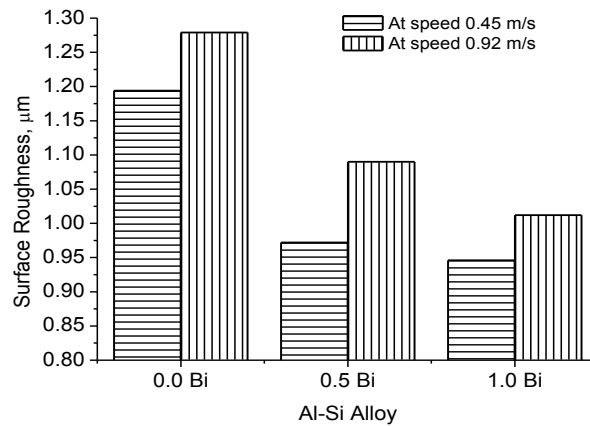


Figure 7. Surface roughness of Al-Si alloy with Bi as cast at cooling rate 9.6°C/s .

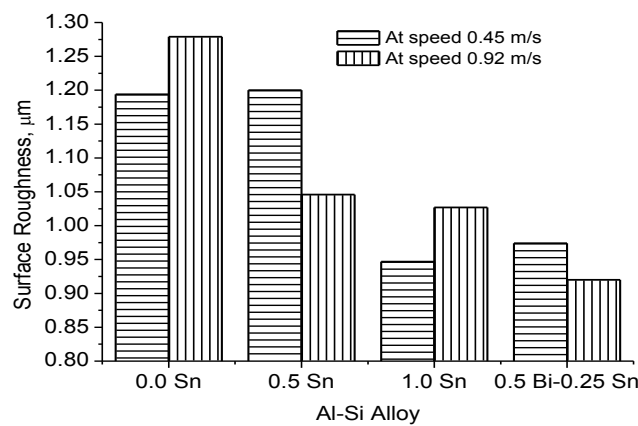


Figure 8. Surface roughness of Al-Si alloy with Sn and Bi+Sn as cast at cooling rate 9.6°C/s .

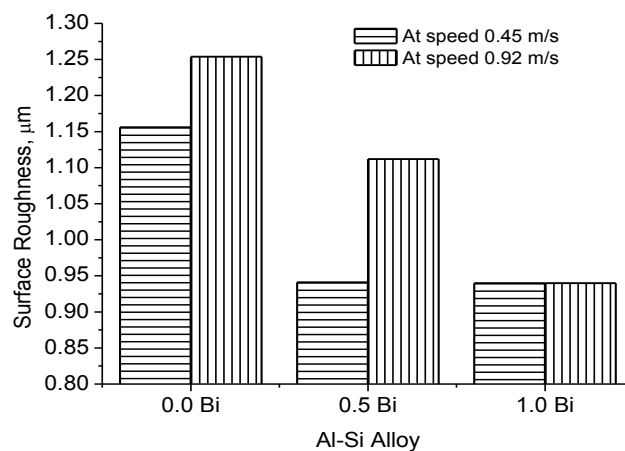


Figure 9. Surface roughness of Al-Si alloy with Bi as cast at cooling rate 26.2°C/s .

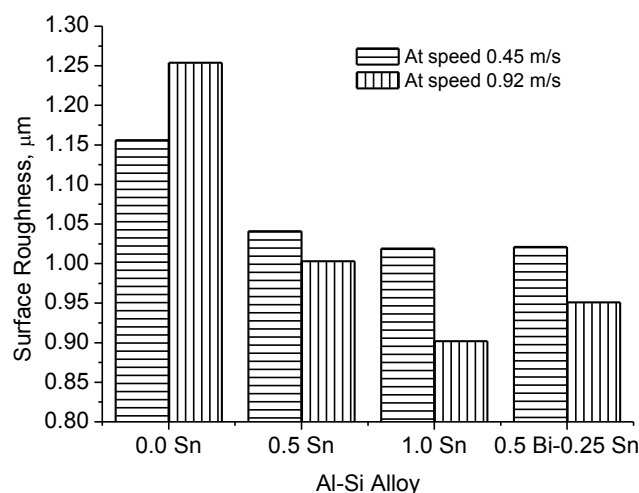


Figure 10. Surface roughness of Al-Si alloy with Sn and Bi+Sn as cast at cooling rate 26.2°C/s.

Alloys Cast At A Cooling Rate 9.6°C/S

The average surface roughness of the Al-Si alloys with different amounts of Sn addition is shown in figures 7 and 8. The average surface roughness was in the range of 0.949 µm to 1.194 µm for the turning speed of 0.45 m/s, and in the range of 1.027 µm to 1.279 µm for the turning speed of 0.92 m/s. While, the average surface roughness with 0.5% Bi + 0.25% Sn was 0.974 µm for the turning speed of 0.45 m/s, and 0.92 µm for the turning speed of 0.92 m/s. So, the Al-Si alloy with 0.5% Bi + 0.25% Sn additions has the smoothest surface and is good for bearing application.

Alloys Cast at a Cooling Rate 26.2°C/s

The average surface roughness of the Al-Si alloys with different amounts of Sn addition was in the range of 1.019 µm to 1.156 µm for the turning speed of 0.45 m/s, and in the range of 0.902 µm to 1.254 µm for the turning speed of 0.92 m/s as shown in figures 9 and 10. While, the average surface roughness with 0.5% Bi + 0.25% Sn was 1.021 µm for the turning speed of 0.45 m/s, and 0.951 µm for the turning speed of 0.92 m/s. So, the Al-Si alloy with 1% Sn addition has the smoothest surface and is good for bearing applications. The surface roughness of the alloys is affected by the turning speed and the cooling rate as shown and discussed. Indeed, low speeds are used for rough cutting and high speeds are employed for fine finishing in the machine shop.

Conclusion

For the Al-Si alloys with different Sn contents as cast at different cooling rates and machined with

different turning speeds, it can be summarized as follows:

1. For the hypoeutectic Al-Si alloy, the eutectic silicon morphology is coarsened with the increase of Bi under the lower cooling rate; the morphology is changed marginally at the higher cooling rate. Sn has no impact on the silicon morphology because it tended to form a film on the boundaries of the Al grains or at the interface of Al and Si.
2. The surface roughness of the alloys is affected by the turning speed.
3. The addition of Sn improved the surface performance of the Al-Si alloys and Al-Si alloys with 1.0% Sn cast at a cooling rate 26.2°C/s at a speed, 0.92 m/s has smoothest surface and is good for bearing applications.

Acknowledgments

My heartfelt gratitude is extended to my wife and my kids for their encouragement, patience and support.

References

- Ammar HR, Samuel AM, Samuel FH, 2008. Effect of casting imperfections on the fatigue life of 319-F and A356-T6 Al-Si casting alloys. *Materials Science and Engineering A*. 473: 65-75.
- Balaji AK, Jawahir IS, 2001. A machining performance study in dry contour turning of aluminum alloys with flat-faced and grooved diamond tools. *Machining Science and Technology*. 5: 269-289.
- Chen P, Hu H, Alpas AT, 2009. Effect of bismuth on the tensile properties and dry machining performance of Al-12.7 wt% Si alloy. *Ceramic Transaction*. 37: 215-223.

- Cho JI, Loper CR, 2000. Limitation of Bismuth residual in A356.2 Al. AFS Trans. 104: 359–367.
- Dasch JM, Ang CC, Wong CA, Waldo RA, Chester D, Cheng YT., Powell BR, Weiner AM, Konca E, 2009. The effect of free-machining elements on dry machining of b319 aluminum alloy. *Journal of Materials Processing Technology*. 209: 4638–4644.
- Vandana J, Rao Ch, Anuradha B, Manan K, 2014. Modification of Die Cast Hypoetetic Al–Si Alloy With Different Sources of Nickel and Its Effect on Mechanical Properties. *International Journal of Science, Environment and Technology*. 3: 492–496.
- Emadi D, Whiting L, Gertsman VY, Sahoo MM, et al, 2006. Effect of Tin on the Mechanical Properties of Aluminum 319 Alloy. AFS Trans. V114 110th Metal casting Congress.
- Totten GE, Mackenzie GEDS, 2003. *Handbook of aluminum: physical metallurgy and processes*. CRC Press. 1063–1103.
- Gruzleski JE, Closset BM, 1990. The treatment of liquid aluminum–silicon alloys. *American Foundrymen’s Society Inc*. 27.
- Elzanaty H, 2015. Effect of Composition on the Microstructure, Tensile and Hardness Properties of Al–xSi Alloys. *Journal of Materials Science & Surface Engineering*. 2: 126–129.
- Jorstad JL, 2006. Future technology in die casting. *Die Casting Engineer*. 50: 18–25.
- Koike J, Miki K, Takahashi H, 2000. Effects of the liquid phase on tensile elongation of Al–Bi alloy. *Mater Sci Eng A*. 285: 158–164.
- Machovec CJ, Zindel JW, Godlewski LA, Buczynski GE, 2000. Determining the effect of Bi&Sr interactions on Si morphology in 319Al. *Modern Casting*. 67: 42–44.
- Miller WS, Zhuang L, Bottema J, Wittebrood AJ, De Smet P, Haszler A, Vieregge A, 2000. Recent development in aluminium alloys for the automotive industry. *Mater Sci Eng A*. 80: 37–49.
- Nouari M, List G, Girot F, Coupard D, 2003. Experimental analysis and optimisation of tool wear in dry machining of aluminium alloys. *Wear*. 255: 1359–1368.
- Patel VP, Prajapati HR, 2012. Microstructural and mechanical properties of eutectic Al–Si alloy with grain refined and modified using gravity die casting and sand casting. *International Journal of Engineering Research and Application*. 2: 147–150.
- Prashanth KG, Scudino S, Klauss HJ, Surreddi KB, Loeber L, Wang Z, Chaubey A K, Kühn U, Eckert J, 2013. Microstructure and mechanical properties of Al–12Si produced by selective laser melting: Effect of heat treatment. *Mater Sci Eng A*. 590: 153–160.
- Rincón E, López H, Cisneros MM, Mancha H, Cisneros MA, 2007. Effect of temperature on the tensile properties of an as-cast aluminum alloy A319. *Mater Sci Eng A*. 12: 452–453.
- Samuel AM, Samuel FH, 1995. Effect of melt treatment, solidification conditions and porosity level on the tensile properties of 319.2 end chill aluminium castings. *J Mater Science*. 30: 4823–4833.
- Tash M, Samuel FH, Mucciardi F, Doty HW, 2007. Effect of metallurgical parameters on the hardness and microstructural characterization of as-cast and heat-treated 356 and 319 aluminum alloys. *Materials Science and Engineering A*. 443: 185–201.
- Wang QG, C. Caceres H, 1998. The fracture mode in Al–Si–Mg casting alloys. *Materials Science and Engineering A*. 241: 72–82.
- Yamagata H, Kasprzak W, Aniolek M, Kurita H, Sokolowski JH, 2008. The effect of average cooling rates on the microstructure of the Al–20% Si high pressure die casting alloy used for monolithic cylinder blocks. *J Mater Proc Techno*. 203: 333–341.